Organic & Biomolecular Chemistry

PAPER

Cite this: *Org. Biomol. Chem.*, 2015, **13**, 5182

Isostructural Re(I)/^{99m}Tc(I) tricarbonyl complexes for cancer theranostics†

Patrique Nunes,[a] Goreti Ribeiro Morais,[a] Elisa Palma,[a] Francisco Silva,[a] Maria Cristina Oliveira,[a] Vera F. C. Ferreira,[a] Filipa Mendes,[a] Lurdes Gano,[a] Hugo Vicente Miranda,[b,c] Tiago F. Outeiro,[b,c,d,e] Isabel Santos[a] and António Paulo*[a]

Received 21st January 2015,
Accepted 26th March 2015

DOI: 10.1039/c5ob00124b

www.rsc.org/obc

Merging classical organic anticancer drugs with metal-based compounds in one single molecule offers the possibility of exploring new approaches for cancer theranostics, *i.e.* the combination of diagnostic and therapeutic modalities. For this purpose, we have synthesized and biologically evaluated a series of Re(I)/^{99m}Tc(I) tricarbonyl complexes (**Re1–Re4** and **Tc1–Tc4**, respectively) stabilized by a cysteamine-based (N,S,O) chelator and containing 2-(4′-aminophenyl)benzothiazole pharmacophores. With the exception of **Re1**, all the Re complexes have shown a moderate cytotoxicity in MCF7 and PC3 cancer cells (IC_{50} values in the 15.9–32.1 μM range after 72 h of incubation). The cytotoxic activity of the Re complexes is well correlated with cellular uptake that was quantified using the isostructural ^{99m}Tc congeners. There is an augmented cytotoxic effect for **Re3** and **Re4** (*versus* **Re1** and **Re2**), and the highest cellular uptake for **Tc3** and **Tc4**, which display a long ether-containing linker to couple the pharmacophore to the (N,S,O)-chelator framework. Moreover, fluorescence microscopy clearly confirmed the cytosolic accumulation of the most cytotoxic compound (**Re3**). Biodistribution studies of **Tc1–Tc4** in mice confirmed that these moderately lipophilic complexes (log $D_{o/w}$ = 1.95–2.32) have a favorable bioavailability. **Tc3** and **Tc4** presented a faster excretion, as they undergo metabolic transformations, in contrast to complexes **Tc1** and **Tc2**. In summary, our results show that benzothiazole-containing Re(I)/^{99m}Tc(I) tricarbonyl complexes stabilized by cysteamine-based (N,S,O)-chelators have potential to be further applied in the design of new tools for cancer theranostics.

Introduction

Many benzothiazole derivatives have shown relevant biological features for drug development, both for diagnostic and therapeutic purposes. This class of compounds has proven to be particularly useful for the design of radioactive probes for nuclear imaging and as cytotoxic drugs for antitumor therapies.[1–3]

For nuclear imaging, 2-arylbenzothiazole derivatives have a crucial role in the development of radioprobes for the *in vivo* detection of β-amyloid (Aβ) aggregates by positron emission tomography (PET) and single-photon emission computed tomography (SPECT).[3] The lead compound in these studies has been the so-called "Pittsburgh compound B" (^{11}C-PIB) (Fig. 1). Studies in Alzheimer's disease (AD) patients validated the usefulness of ^{11}C-PIB as a PET imaging probe for Aβ detec-

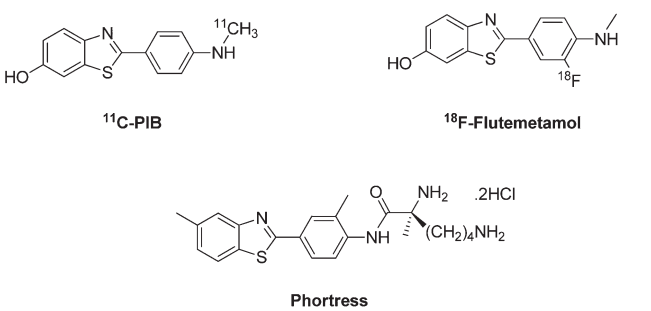

Fig. 1 Chemical structures of clinically relevant benzothiazole derivatives.

[a]*Centro de Ciências e Tecnologias e Nucleares, IST, Universidade de Lisboa, Estrada Nacional 10, 2695-066 Bobadela LRS, Portugal. E-mail: apaulo@ctn.ist.utl.pt*
[b]*Instituto de Medicina Molecular, Av. Prof. Egas Moniz, 1649-028 Lisboa, Portugal*
[c]*CEDOC, Faculdade de Ciências Médicas, Universidade Nova de Lisboa, Lisboa, Portugal*
[d]*Instituto de Fisiologia, Faculdade de Medicina da Universidade de Lisboa, Lisboa, Portugal*
[e]*Department of NeuroDegeneration and Restorative Research, University Medical Center Göttingen, Waldweg 33, 37073 Göttingen, Germany*
†Electronic supplementary information (ESI) available. See DOI: 10.1039/c5ob00124b

tion. However, ^{11}C-PIB is not approved for clinical use.[4,5] Nevertheless, structurally related ^{18}F-labeled congeners, such as ^{18}F-flutemetamol (Fig. 1), have been recently approved by the US Food and Drug Administration (FDA) and European Medicine Agency (EMA) for the visual detection of Aβ burden in patients suspected of AD.[6] Several metal-based compounds bearing arylbenzothiazole moieties were also evaluated for *in vivo* imaging of Aβ plaques. This included the study of ^{99m}Tc complexes for SPECT imaging and Gd complexes as contrast agents for magnetic resonance imaging (MRI).[7–9] The results for metallic complexes were less encouraging if compared with purely organic molecules, reflecting their poor ability to penetrate the blood–brain barrier and to reach the β-amyloid plaques.

The 2-arylbenzothiazole scaffold is also promising for the development of anticancer drugs. It was shown that such a simple scaffold might afford possible drug candidates upon the introduction of minor functional group changes in its core. Many benzothiazole derivatives have demonstrated activity against a wide range of human tumor cell lines, including ovarian, breast, prostate lung, renal, and colon cancer cell lines.[10–13] From a large number of tested molecules, the most explored as an antitumour agent is Phortress (Fig. 1), a 2-(4′-aminophenyl)benzothiazole derivative that underwent a Phase 1 clinical trial.[10]

Merging classical organic anticancer drugs with metal-based compounds in one single molecule offers the possibility of exploring new approaches for cancer theranostics, based on the combination of diagnostic and therapeutic modalities. The metal fragments might confer advantages as theranostic tools, such as the possibility of exploring a larger diversity of chemical structures, which may increase their bioavailability and resistance to metabolic transformation. For this purpose, a large variety of d and f transition metals with nuclear or magnetic properties suitable for medical imaging is available, for example the aforementioned Tc and Gd.[14,15]

In the particular case of technetium, non-radioactive Re complexes are often used as reference compounds to assign the chemical identity of the ^{99m}Tc congeners due to the similitude of the chemistry of these two group 7 elements.[14] Hence, when designing metal-based cancer theranostic agents, the Re complexes can be incorporated into the cytotoxic entity that will exert a therapeutic effect while the ^{99m}Tc congeners are part of the imaging entity that will enable the *in vivo* detection of tumor tissues. In addition, there are two beta-emitting radioisotopes of rhenium (^{186}Re and ^{188}Re) that present physical properties suitable for radionuclide therapy.[14] Therefore, Tc and Re can be seen as a unique match-pair of d-transition elements that enables the design of radiopharmaceuticals for diagnostic (^{99m}Tc) and therapeutic applications ($^{186/188}$Re), offering further possibilities for cancer theranostics by allowing the combination of SPECT imaging with chemo- and/or radiotherapeutic modalities.

Recently, the 2-(4′-aminophenyl)benzothiazole pharmacophore was linked to acyclic or macrocyclic bifunctional chelators (BFCs), which were used to obtain ^{99m}Tc(I) tricarbonyl complexes and Gd(III) complexes. These complexes were evaluated as SPECT- or MRI-imaging compounds for cancer theranostics, respectively.[16–18] These first studies led to encouraging biological results underlying the relevance of benzothiazole-containing metal complexes in this field of research. In this context, we have embarked on the synthesis and biological evaluation of new benzothiazole-containing ^{99m}Tc(I) and Re(I) tricarbonyl complexes stabilized by a (S,N,O)-donor BFC derived from cysteamine. Here, we report on the synthesis and characterization of these new complexes, as well as on their biological evaluation as potential cancer theranostic agents. For the Re complexes, the biological evaluation comprised the assessment of their cytotoxic activity against human breast cancer – MCF7 – and prostate cancer – PC3 – cell lines using the 3-(4,5-dimethylthiazol-2-yl)-2,5-diphenyltetrazolium bromide (MTT) assay, and the visualization of cellular uptake by fluorescence microscopy. Conversely, the ^{99m}Tc counterparts were used for the quantification of the uptake in the same cell lines, and to ascertain the biodistribution and *in vivo* stability of the complexes in mice.

Results and discussion

Synthesis and characterization of the ligands

As mentioned above, we have considered (S,N,O)-donor BFCs derived from cysteamine to stabilize the *fac*-$[M(CO)_3]^+$ (M = Re, ^{99m}Tc) core and to be functionalized with the 2-(4′-aminophenyl)benzothiazole pharmacophore. In the last few years, this core has gained an increasing impact in radiopharmaceutical chemistry following the introduction by Alberto and coworkers of a convenient and fully aqueous-based kit preparation of the organometallic precursors *fac*-$[M(OH_2)_3(CO)_3]^+$.[19,20] This so-called tricarbonyl approach has several intrinsic advantages, including the high stability and kinetic inertness inherent to Tc(I) and Re(I) tricarbonyl complexes when appropriate ligands are used.[21] Previously, we have shown that the cysteamine-based (S,N,O)-donor ligand 2-(2-(ethylthio)ethylamino)acetic acid affords low-molecular weight and lipophilic ^{99m}Tc(I)/Re(I) complexes with high *in vitro* and *in vivo* stability.[22,23] We have anticipated that the replacement of the S-terminal ethyl substituent of this chelator by the 2-(4′-aminophenyl)benzothiazole pharmacophore would not compromise the coordination capability of the (S,N,O)-donor set towards *fac*-$[M(CO)_3]^+$ (M = Re, ^{99m}Tc) and the biological properties of the pharmacophore.

Four new BFCs, **L1–L4**, were synthesized by linking 2-arylbenzothiazole pharmacophores to the 3-((2-mercaptoethyl)-amino)propanoic acid coordinating unit by using two different aliphatic spacers, displaying or not an ether function (Schemes 1 and 2). The synthesis of **L1–L4** has been achieved in a convergent way, using compounds **3** and **4** as common intermediates. As depicted in Scheme 1, the 2-aryl benzothiazole rings of **3** and **4** were formed through cyclocondensation of the *o*-aminothiophenols **1** and **2**, by reaction with the adequate *N*-substituted benzaldehyde under basic conditions. For **L1** and **L2**, which do not contain any ether function in their

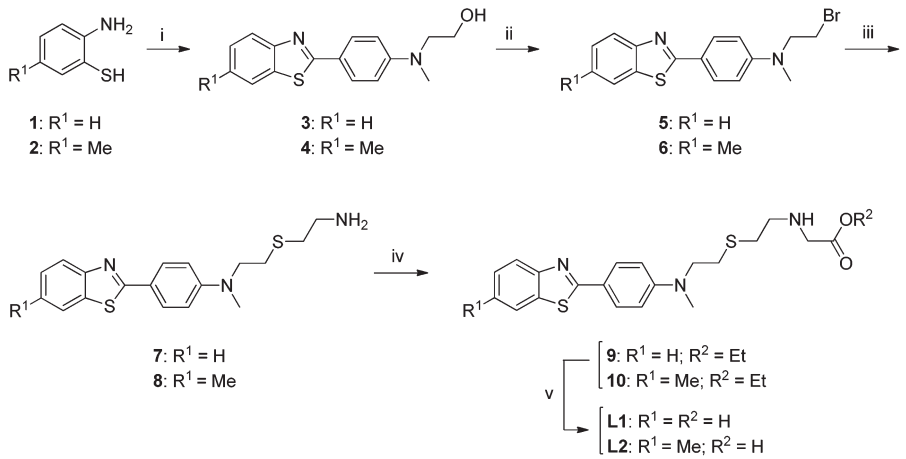

Scheme 1 Synthetic route for the preparation of ligands **L1** and **L2**. Conditions: (i) *N*-methyl-*N*-(2-hydroxyethyl)-4-aminobenzaldehyde, pyridine, reflux; (ii) CH_2Cl_2, CBr_4, PPh_3, RT; (iii) NaOH, EtOH, 2-aminoethanethiol hydrochloride, RT; (iv) CH_3CN, KI, K_2CO_3, ethyl 2-bromoacetate, reflux; (v) THF, water, NaOH, reflux.

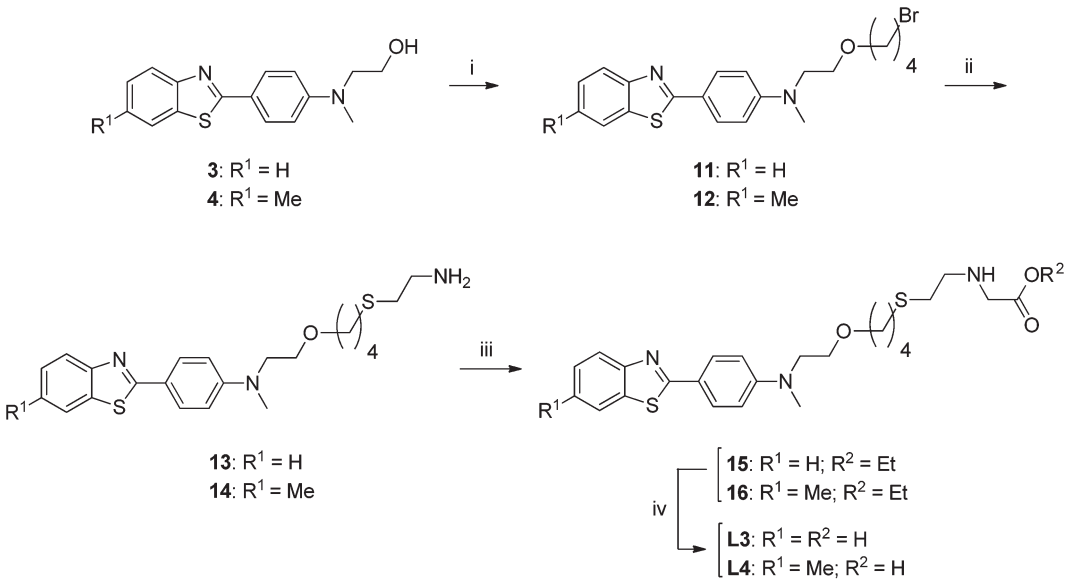

Scheme 2 Synthetic route for the preparation of **L3** and **L4**. Conditions: (i) THF, NaH, 1,4-dibromobutane; (ii) NaOH, EtOH, 2-aminoethanethiol hydrochloride, RT; (iii) CH_3CN, KI, K_2CO_3, ethyl 2-bromoacetate, reflux; (iv) THF, water, NaOH, reflux.

structure, the synthesis involved the brominated derivatives **5** and **6** as intermediates. Compounds **5** and **6** were obtained in moderate yield (η = 56–64%) from the benzothiazoles **3** and **4** using the Appel reaction (Scheme 1). The synthesis of **L3** and **L4**, having an ether function in the linker between the pharmacophore and the S,N,O-coordinating unit, was also achieved using brominated intermediates (compounds **11** and **12**); **11** and **12** were obtained in good yield (η = 40–45%) by the O-alkylation of **3** and **4** with an excess of 1,4-dibromobutane (Scheme 2). For all the ligands, the incorporation of the benzothiazole moieties into the (S,N,O)-donor coordination unit was accomplished in a sequential manner, in which the brominated derivatives **5**, **6**, **11**, and **12** acted as electrophiles in S-alkylation reactions of 2-aminoethanethiol, followed by the N-alkylation of the resulting compounds (**7**, **8**, **13**, and **14**, respectively) with ethyl bromoacetate. Finally, basic hydrolysis of the obtained benzothiazole ester derivatives (**9**, **10**, **15**, and **16**, respectively) gave the ligands **L1–L4**. All the compounds were characterized using common spectroscopy techniques (^{1}H and ^{13}C NMR) and by ESI-MS, which confirmed the proposed formulations.

Synthesis and characterization of the organometallic Re and ^{99m}Tc complexes

The synthesis of the Re(I) tricarbonyl complexes **Re1–Re4** was performed by ligand exchange reactions of *fac*-

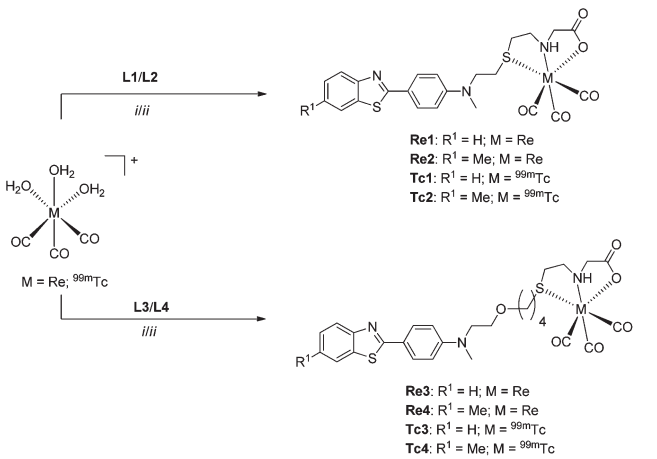

Scheme 3 Synthesis of the Re(I) and ^{99m}Tc(I) tricarbonyl complexes. Conditions: (i) $[Re(H_2O)_3(CO)_3]Br$, methanol, reflux, 16 h; (ii) $[^{99m}Tc(H_2O)_3(CO)_3]$, H_2O, 100 °C, 30 min.

$[Re(H_2O)_3(CO)_3]Br$ with **L1–L4** in refluxing methanol (Scheme 3). After adequate purification, complexes **Re1–Re4** were recovered as yellow microcrystalline solids in moderate to high yield (57–81%). Their characterization was performed using common spectroscopy techniques (IR, ^{1}H and ^{13}C NMR), ESI-MS, HPLC and elemental analysis.

The positive ESI mass spectra obtained for **Re1–Re4** showed the presence of prominent peaks corresponding to the respective $[M + H]^+$ molecular ions; unlike **Re1** and **Re2**, intense peaks that were assigned to $[M + Na]^+$ were also observed in the mass spectra of **Re3** and **Re4**. This difference certainly reflects the presence of an ether function in the aliphatic spacers of **L3** and **L4**, which might enhance the interaction with the sodium cation. The IR spectroscopic data obtained for all the complexes corroborated the presence of the *fac*-$[Re(CO)_3]^+$ core, detecting two strong bands assignable to ν(C≡O) in the 1893–2028 cm^{-1} range. Moreover, the HPLC analysis of **Re1–Re4** showed that the complexes were of high purity, as only single peaks were detected in the respective chromatograms.

The chemical characterization of **Re1–Re4** by NMR spectroscopy was more demanding. At room temperature, the ^{1}H NMR spectra of these complexes in DMF-d_7 displayed a set of relatively broad and ill-defined resonances in the area of the methylenic and methyl protons, ranging from 1.71 to 3.96 ppm. The aromatic protons from the 2-(4′-aminophenyl)-benzothiazole pharmacophore gave rise to better defined and well resolved signals that appear between 6.90 and 8.10 ppm. The broadness of the resonances from the aliphatic protons suggested that complexes **Re1–Re4** undergo dynamic processes in solution, as confirmed for **Re1** by variable temperature ^{1}H NMR studies (Fig. 2). The dynamic behavior observed for **Re1–Re4** is most probably due to the occurrence of pyramidal inversion at the coordinated sulfur atom, as we have previously observed for the congener Re(I) tricarbonyl complex with 2-(2-(ethylthio)ethylamino)acetic acid (herein designated as **Re(CO)$_3$(NSO)**).[22] These findings indicate that **Re1–Re4** most probably contain ligands coordinated in a N,S,O-tridentate fashion, a coordination mode that was confirmed by X-ray diffraction analysis in the case of **Re(CO)$_3$(NSO)**.[23]

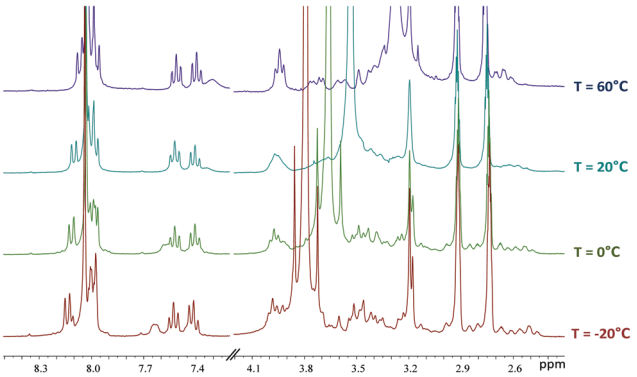

Fig. 2 ^{1}H NMR spectra of complex **Re1** at various temperatures in DMF-d_7.

In aqueous solution and at 100 °C, **L1–L4** readily reacted with *fac*-$[^{99m}Tc(CO)_3(OH_2)_3]^+$ affording complexes **Tc1–Tc4**, respectively (Scheme 3). The reactions are almost quantitative (>95%) for final concentrations of **L1–L4** as low as 10^{-4} M, complexes **Tc1–Tc4** being the unique species formed. Their chemical identity was confirmed by comparison of their HPLC profiles with those of the corresponding rhenium complexes, as exemplified for **Tc1**/**Re1** in Fig. 3.

The characterization of **Tc1–Tc4** comprised also the evaluation of their lipophilicity, which was assessed by the measurement of the respective log $D_{o/w}$ values (*n*-octanol/0.1 M, phosphate buffered saline (PBS), pH 7.4) using the "shake-flask" method. The log $D_{o/w}$ values and the HPLC retention times of **Tc1–Tc4** are shown in Table 1. All the complexes are moderately lipophilic with log $D_{o/w}$ values spanning in a rather narrow range, from 1.98 to 2.32, suggesting that the presence of the ether linkage balances the increase of lipophilicity

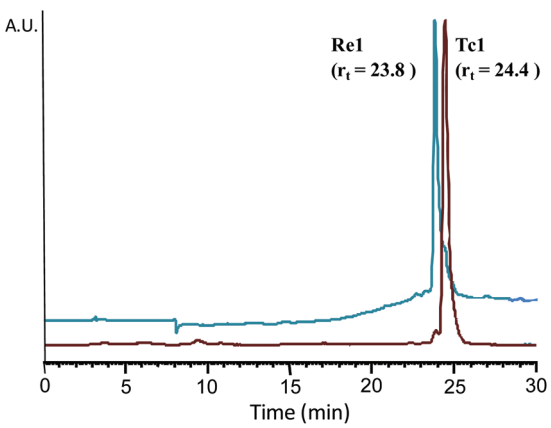

Fig. 3 HPLC chromatograms of complexes **Re1** (UV detection) and **Tc1** (radiometric detection).

Table 1 HPLC retention times and log $D_{o/w}$ of complexes **Tc1–Tc4**

Complex	$r_t^{a,b}$ (min)	log $D_{o/w}$
Tc1	24.4 (23.8)	1.98 ± 0.02
Tc2	24.9 (24.1)	2.01 ± 0.05
Tc3	24.0 (23.3)	1.95 ± 0.01
Tc4	26.0 (25.9)	2.32 ± 0.04

[a] Using a gradient of aqueous 0.1% CF_3COOH and methanol as the solvent. [b] The values in parentheses are the retention times for the Re congeners.

caused by the larger number of methylenic groups in the linker.

Biological evaluation of the Re complexes: cytotoxicity assays and microscopy studies

The cytotoxic activity of the ligands and respective Re complexes was tested on human breast cancer – MCF7 – and prostate cancer – PC3 – cell lines. These cancer cells were treated with decreasing concentrations (200–0.002 μM) of the different compounds and incubated for 72 h at 37 °C. All the tested compounds were first solubilized in DMSO and diluted in the cell media. The percentage of DMSO never exceeded 1%, a non-toxic concentration. After the treatment, the cellular viability was assessed by the MTT assay. The inhibition of growth (%) was calculated by correlation with vehicle-treated cells. The IC_{50} values, expressed in μM concentrations, are average ± standard deviations of 3 independent experiments with 4 replicates each, and the results are presented in Table 2.

In general, the complexes **Re2–Re4** exhibited higher cytotoxicity than the respective ligands **L2–L4** in the MCF7 breast and PC3 prostate cell lines. In contrast, in these cell lines **L1** is more cytotoxic than **Re1**. From all the studied compounds, the complexes **Re3** and **Re4** were shown to be the most potent, with IC_{50} values between 15.9 ± 1.1 and 32.1 ± 1.2 μM in both cell lines.

Taking advantage of the fluorescence emission characteristics of the benzothiazole unit of the newly synthesized compounds, the cellular uptake of the most cytotoxic Re complex, **Re3**, was assessed by fluorescence microscopy in MCF7 and PC3 human cancer cells. For comparative purposes, the studies were also performed for the respective ligand **L3**. Compounds **L3** and **Re3** were detected by the emission of blue fluorescence and the nucleus stained with propidium iodide (red emission).

As shown in Fig. 4, both complexes **Re3** and **L3** (to a lesser extent) were detected in the cytoplasm of both cell lines. No detectable fluorescence in the blue channel was observed for the DMSO control, confirming that the detected blue emission is from the compounds **L3** and **Re3**, and not due to the unspecific signal.

The cell entrance/uptake seems to be reduced for **L3** when compared with **Re3**, as less fluorescence was detected from cells incubated with **L3** if compared with those incubated with **Re3**. It is important to mention that in Fig. 4 all the images were collected using the same conditions, in particular the acquisition time. A second set of images was collected with a longer acquisition time to further evaluate the cellular uptake and localization of **L3** (Fig. 5), showing intracellular cytoplasmic accumulation.

In addition, the fluorescence spectra obtained for **L3** and **Re3** (at the same concentration) have shown no detectable differences in the maximum wavelength of excitation and emission (Fig. 5). Moreover, these experiments have shown that **L3** is a slightly more efficient fluorophore than **Re3**. Hence, the more intense fluorescence detected in the cells incubated with **Re3** is not due to its intrinsic fluorescence

Table 2 Cytotoxicity of **L1–L4** and **Re1–Re4** in MCF7 breast and PC3 prostate cancer cells

	$IC_{50}{}^a$ (μM)	
Compound	MCF7	PC3
L1	25.6 ± 1.4	32.5 ± 1.1
Re1	90 ± 1.2	94 ± 1.3
L2	241 ± 1.8	89 ± 1.1
Re2	30.7 ± 1.0	30.6 ± 1.0
L3	52.2 ± 1.1	95 ± 1.2
Re3	15.9 ± 1.1	28.8 ± 1.1
L4	39.3 ± 1.1	71.3 ± 1.1
Re4	16.3 ± 1.2	32.1 ± 1.2

[a] IC_{50}: the concentration that causes 50% reduction of the cell growth.

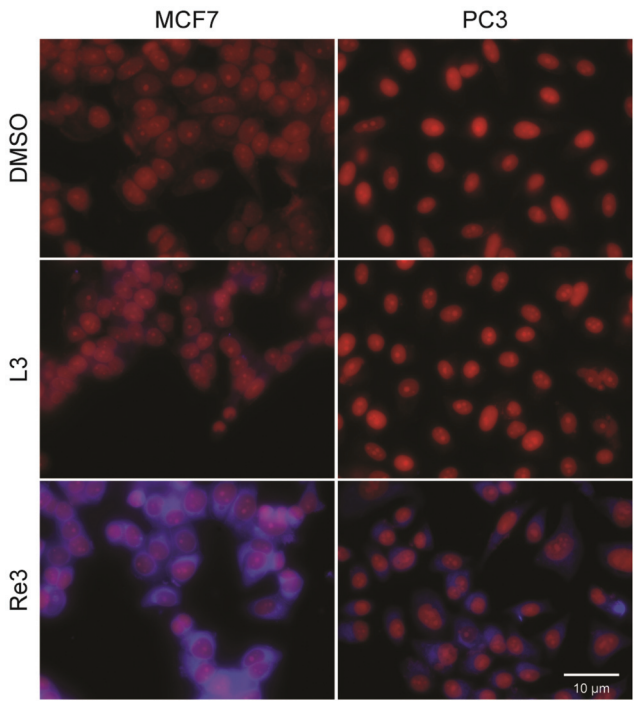

Fig. 4 Fluorescence microscopy evaluation of the uptake of **L3** and **Re3** (blue) in human MCF7 and PC3 cells. Nuclei (red) were stained with propidium iodide. Scale bar, 10 μm.

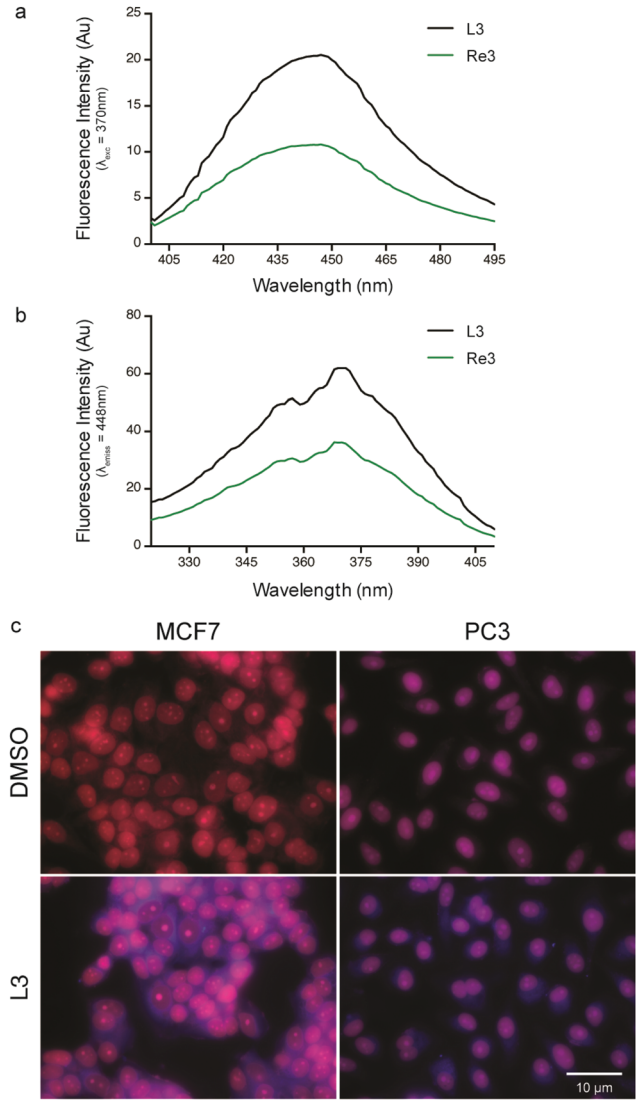

Fig. 5 Emission and excitation spectra of **L3** (a) and **Re3** (b). Fluorescence microscopy evaluation of human MCF7 and PC3 cancer cell uptake of L3 (blue) (c). Nuclei (red) were stained with propidium iodide. Note: images were collected with higher acquisition times than those presented in Fig. 4. Scale bar, 10 μm.

properties. Altogether, these data indicate that **Re3** is able to enter into cancer cell lines more easily than the corresponding ligand **L3**. Eventually, this might explain the highest cytotoxicity that has been found for **Re3** in the MCF7 and PC3 cancer cell lines, in comparison with the respective ligand.

Biological evaluation of ^{99m}Tc complexes: cellular uptake and biodistribution studies

The microscopy studies performed for **Re3** have confirmed that this complex can reach the cytoplasm of MCF7 breast and PC3 prostate human cancer cells. The isostructural ^{99m}Tc complex, **Tc3**, was used to quantify the cellular uptake in the same cell lines. These studies were extended to the other radioactive complexes (**Tc1**, **Tc2** and **Tc4**) aiming to correlate their cellular uptake with the cytotoxicity exhibited by the corresponding Re complexes. The breast and prostate cancer cell lines were treated with **Tc1–Tc4** for different times (0 to 18 h) and the results show that complexes **Tc1–Tc4** display a high cellular uptake in both cell lines, in a time-dependent manner, with values at 18 h in the range of 14–29% and 23–48% for MCF7 and PC3 cells, respectively (Fig. 6). The highest uptake was observed in the PC3 cells, in particular for the complexes **Tc3** and **Tc4** with values of 38.6% and 31.5% at 5 h and values of 47.1% and 47.9% at 18 h, respectively. These results demonstrate that the complexes **Tc3** and **Tc4** display the highest cellular uptake in the MCF7 and PC3 cells, accumulating in both cell lines over time. This trend seems to be in agreement with the highest cytotoxicity of the Re congeners (**Re3** and **Re4**), particularly in the MCF7 breast cancer cell line.

As discussed before, all complexes are lipophilic with $\log D_{o/w}$ values within the relatively narrow range of 1.98–2.32. Therefore, the lipophilicity is not expected to be the major cause of the large differences observed between the cellular uptake of **Tc1–Tc4**. This is clearly corroborated by the fact that **Tc1** ($\log P$ = 1.98 ± 0.02) and **Tc3** ($\log P$ = 1.95 ± 0.02), having almost equal $\log P$ values, present a large difference in the cellular uptake values, which for **Tc3** is as high as 30.9% of the applied activity/million cells in the PC-3 cell line *versus* 13.3% for **Tc1** at 5 h.

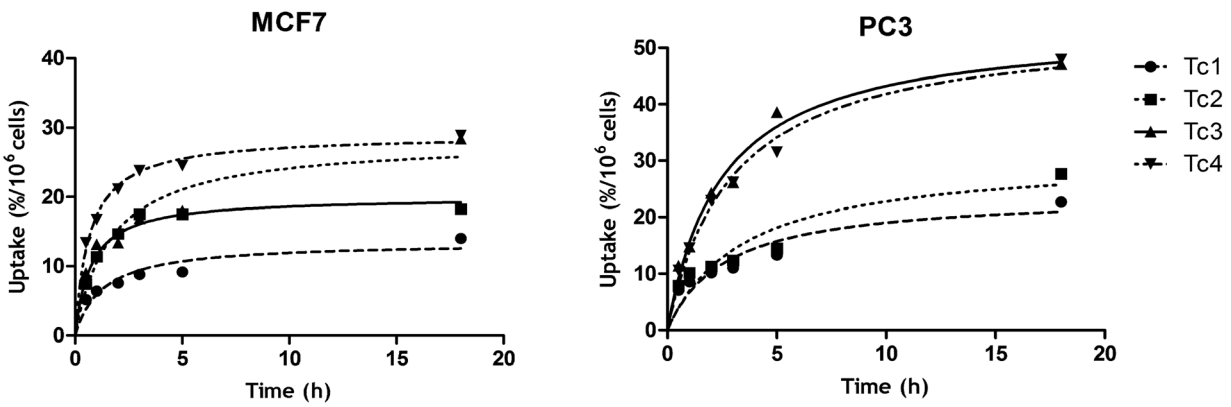

Fig. 6 Cellular uptake of **Tc1–Tc4** in human MCF7 breast and PC3 prostate cells, expressed as a percentage of total radioactivity per million cells.

Table 3 Biodistribution data (%ID g^{-1}) of **Tc1–Tc4** at 2 and 60 min post-injection (p.i.) in CD-1 mice

	% ID g^{-1} ± SD							
	Tc1		**Tc2**		**Tc3**		**Tc4**	
Organ	2 min	60 min	2 min	60 min	2 min	60 min	2 min	60 min
Blood	6.40 ± 1.10	0.58 ± 0.11	7.00 ± 0.50	1.00 ± 0.09	8.00 ± 2.40	0.70 ± 0.20	5.20 ± 0.90	0.84 ± 0.05
Liver	43.3 ± 1.90	37.5 ± 1.60	19.9 ± 2.60	15.2 ± 2.40	35.8 ± 1.60	11.3 ± 1.20	35.8 ± 4.40	29.5 ± 0.60
Intestine	3.10 ± 0.40	19.5 ± 1.70	1.40 ± 0.40	11.5 ± 3.20	3.90 ± 0.50	10.3 ± 1.20	2.40 ± 0.30	17.2 ± 0.50
Spleen	3.90 ± 0.20	0.50 ± 0.20	3.70 ± 0.03	0.78 ± 0.01	2.90 ± 0.60	0.26 ± 0.03	5.20 ± 0.90	0.70 ± 0.10
Heart	5.40 ± 0.60	0.90 ± 0.30	3.80 ± 0.70	0.90 ± 0.10	3.70 ± 0.80	0.42 ± 0.08	4.40 ± 0.20	1.10 ± 0.20
Lungs	7.00 ± 1.00	1.10 ± 0.20	13.9 ± 0.70	3.00 ± 0.80	3.50 ± 1.00	0.70 ± 0.20	9.00 ± 1.00	3.70 ± 0.60
Kidney	21.6 ± 2.90	2.70 ± 0.20	11.8 ± 4.20	1.90 ± 0.80	14.9 ± 2.20	2.00 ± 0.50	13.2 ± 0.70	2.10 ± 0.40
Muscle	1.20 ± 0.20	0.60 ± 0.10	0.90 ± 0.30	0.55 ± 0.08	0.80 ± 0.30	0.29 ± 0.07	1.40 ± 0.10	0.67 ± 0.06
Skeletal	1.50 ± 0.20	0.46 ± 0.09	1.30 ± 0.30	0.45 ± 0.06	1.40 ± 0.20	0.19 ± 0.03	1.96 ± 0.07	0.54 ± 0.04
Stomach	1.20 ± 0.40	2.60 ± 0.70	0.69 ± 0.10	1.30 ± 0.30	0.90 ± 0.60	1.50 ± 0.50	1.80 ± 0.50	3.60 ± 0.70
Brain	0.30 ± 0.08	0.03 ± 0.01	0.19 ± 0.04	0.04 ± 0.00	0.20 ± 0.04	0.02 ± 0.01	0.40 ± 0.10	0.05 ± 0.01
Excretion (% IA)		2.70 ± 0.50		3.60 ± 2.40		18.4 ± 1.70		12.4 ± 3.40

The most striking structural differences in complexes **Tc1–Tc4** are related to the linkers used to attach the 2-arylbenzothiazole pharmacophore to the 3-((2-mercaptoethyl)amino)-propanoic acid coordinating unit. A shorter ethylenic linker has been used in complexes **Tc1** and **Tc2**, which have shown a much lower cellular uptake than **Tc3** and **Tc4**, containing a longer 2-*n*-butoxyethyl linker. The use of a longer linker is expected to minimize the interference of the organometallic fragment in molecular interactions involving the pharmacophore and biologically relevant targets. It is worthwhile mentioning that many benzothiazole derivatives like the parent compound 2-(4′-aminophenyl)-benzothiazole and its derivatives bearing 3′ substituents undergo a selective uptake and biotransformation only in sensitive cancer cell lines, such as MCF-7 breast cancer cells. In these sensitive cell lines, the compounds bind to the aryl hydrocarbon receptor (AhR) with AhR translocation to the nucleus and subsequent induction of the expression and activation of the cytochrome P450 isoform CYP1A1. In contrast, insensitive cells like the prostate carcinoma PC3 cells do not show AhR translocation and CYP1A1 activation upon treatment with the same benzothiazole derivatives.[12,13,24] We did not fully investigate the mechanisms involved in the cellular uptake of **Tc1–Tc4** and in the cytotoxic activity of the congener **Re1–Re4**, but the higher uptake observed for the ^{99m}Tc complexes in the PC3 cell line in comparison with the MCF7 cell line and similar cytotoxic activity of the Re complexes in both cell lines indicate that the interaction with AhR is most likely not responsible for the biological activity exhibited.

Finally, biodistribution studies of complexes **Tc1–Tc4** were performed in CD-1 mice to assess their pharmacokinetic profile and *in vivo* stability. The biodistribution data obtained for **Tc1–Tc4** at 2 min and 1 h post intravenous injection (p.i.), expressed in percent of the injected dose per gram of tissue (%ID g^{-1}), are presented in Table 3.

All complexes show a relatively fast blood clearance but a rather low rate of excretion that varied between 2.70 and 18.4% I.A. At 1 h p.i., most of the activity is retained in the liver and intestine due to the predominantly hepatobiliary excretion of these moderately lipophilic compounds. Despite their neutrality and lipophilicity, **Tc1–Tc4** showed a negligible brain uptake (<0.40% ID g^{-1}) confirming their inability to cross the blood–brain barrier in mice.

The *in vivo* stability of **Tc1–Tc4** has been assessed by HPLC analysis of the urine and plasma of mice injected with these complexes. At 2 min p.i., most of the radioactivity detected in the plasma corresponds to the intact complexes (Fig. 7). However, the complexes with an ether-containing longer linker, **Tc3** and **Tc4**, have a higher tendency to undergo metabolic transformations, as indicated by the HPLC chromatograms obtained for the plasma at 1 h p.i. As exemplified for **Tc4** in Fig. 7, a significant part of the circulating activity still corresponds to the intact complex but two metabolites were detected at retention times of 17.2 and 18.7 min, respectively. These metabolites are also the major radiochemical species that are present in the HPLC chromatograms of the urine of mice injected with **Tc4**, at 1 h p.i. (data not shown). We did not identify these metabolites but their formation might be related to transformations involving the ether function from the aliphatic linker used to couple the benzothiazole pharmacophore with the (N,S,O) chelator framework in complexes **Tc3** and **Tc4**. For instance, the ether function can be involved in O-dealkylation processes, followed by oxidation of the resulting alcohol functions, as we have recently shown for ^{99m}Tc(I) tricarbonyl complexes with ether-containing pyrazolyl derivatives.[25] The formation of these metabolites *in vivo* can certainly justify that complexes **Tc3** and **Tc4** display a faster excretion rate than **Tc1** and **Tc2**.

Conclusions

The functionalization of the 3-((2-mercaptoethyl)amino)propanoic acid coordinating unit with the 2-(4′-aminophenyl)benzo-

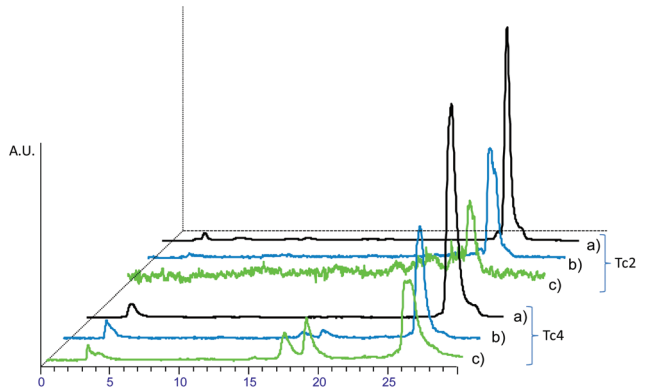

Fig. 7 *In vivo* stability studies of complexes **Tc2** and **Tc4**. HPLC chromatograms of: (a) injected preparation; (b) plasma collected at 2 min p.i.; (c) plasma collected at 1 h p.i.

thiazole pharmacophore, using two different aliphatic spacers containing or not an ether function, led to a new family of benzothiazole-containing chelators: **L1–L4**. These chelators were successfully applied in the synthesis of M(I) (M = Re, ^{99m}Tc) tricarbonyl complexes (**Re1–Re4** and **Tc1–Tc4**), which were biologically evaluated as isostructural tools for cancer theranostics.

The Re complexes have shown a moderate cytotoxic activity against PC3 and MCF7 human tumor cells (IC_{50} values <50 μM after 72 h of incubation), with the exception of **Re1** that showed relatively high IC_{50} values (>50 μM). In general, the Re complexes are more cytotoxic than the corresponding ligands, which is most probably due to the better ability of the complexes to enter into the cells, as confirmed by fluorescence microscopy studies in the case of **Re3**/**L3**.

There is a clear influence of the linker on the cytotoxicity of the complexes, those which display the ether-containing linker, *i.e.* **Re3** and **Re4**, being the most active. The cytotoxicity activity of the Re complexes is well correlated with the cellular uptake, which has been quantified using the ^{99m}Tc congeners, **Tc1–Tc4**. Interestingly, the nature of the linker also strongly influences the *in vivo* behavior of the complexes, as **Tc3** and **Tc4** are more prone to metabolic transformations and display a faster excretion rate in mice.

In summary, the moderate cytotoxicity exhibited by the Re complexes, together with the remarkably high cellular uptake and the reasonably good bioavailability presented by the ^{99m}Tc congeners, show that the benzothiazole-containing Re(I)/^{99m}Tc(I) tricarbonyl complexes described here hold promise to be further applied in the design of new tools for cancer theranostics. The marked influence of the linker on the biological fate of the complexes and its easy structural modification, as well as the different possibilities available to attach the 2-(4′-aminophenyl)benzothiazole pharmacophore (*e.g.* N-alkylation *vs.* amide-forming reactions) to the cysteamine based (N,S,O)-chelator are expected to help in the search for better performing compounds and on the elucidation of structure–activity relationships (SAR).

Experimental section

General information

All chemicals and solvents were of reagent grade and were used without purification unless stated otherwise. 2-Amino-5-methylbenzenethiol (**2**) was prepared as described in the literature.[26] *fac*-$[Re(H_2O)_3(CO)_3]Br$ was synthesized according to the literature.[27] Na[$^{99m}TcO_4$] was eluted from a commercial ^{99}Mo/^{99m}Tc generator, using a 0.9% saline solution. The *fac*-$[^{99m}Tc(H_2O)_3(CO)_3]^+$ precursor was obtained by labelling of a Isolink®-kit with Na[$^{99m}TcO_4$], following the procedure described elsewhere.[20] The NMR spectra were recorded on a Varian Unity 300 NMR spectrometer at frequencies of 300 MHz (^{1}H) and 75 MHz (^{13}C). Chemical shifts are reported in parts per million. ^{1}H and ^{13}C NMR chemical shifts were referenced with the residual solvent resonances relative to tetramethylsilane. FTIR spectra were recorded using KBr pellets on a Bruker, Tensor 27 spectrometer. Electrospray ionisation mass spectrometry (ESI-MS) was performed on a QITMS instrument in positive and negative ionization mode. Thin-layer chromatography (TLC) was performed on precoated silica plates 60 F_{254} (Merck). Visualization of the plates was carried out using UV light (254 and 365 nm) and/or an iodine chamber. Gravity column chromatography was carried out on silica gel (Merck, 70–230 mesh). HPLC analysis of the Re and ^{99m}Tc complexes was performed on a PerkinElmer LC pump coupled to an LC tuneable UV/Vis detector and to a Berthold LB-507A radiometric detector, using an analytical C18 reversed-phase column (Nucleosil 100-10, 250 × 3 mm) with a flow rate of 1 ml min^{-1}. UV detection, 254 nm. Eluents: A – aqueous 0.1% CF_3COOH solution, B – MeOH. The HPLC analysis was performed with gradient elution, using the following method: 0–8 min, 100% A; 8–8.1 min, 100%–75% A; 8.1–14 min, 75% A; 14–14.1 min, 75%–66% A; 14.1–25 min, 66%–0% A; 25–30 min, 0% A; 30–30.1 min, 0–100% A; 30.1–35 min, 100% A.

Synthesis of the ligands

2-[*N*-Methyl-*N*-(2′-hydroxyethyl)-4′-aminophenyl]-benzothiazole (3). A solution of *o*-aminothiophenol (557 mg, 4.5 mmol) and *N*-methyl-*N*-(2-hydroxyethyl)-4-aminobenzaldehyde (660 mg, 3.7 mmol) in pyridine (6 mL) was refluxed for 3 h. After cooling at room temperature the intense yellow suspension was neutralized with a 3 M HCl solution and the solvent was concentrated. The reaction crude was taken in water (50 mL) and extracted with CH_2Cl_2 (3 × 30 ml). The organic phase was dried over Na_2SO_4, filtered and evaporated. The residue was subjected to column chromatography on silica-gel (CH_2Cl_2–MeOH, 98 : 2) to give **3** (510 mg, 49%); R_f = 0.25 (*n*-hexane–AcOEt 1 : 1); ^{1}H NMR ($CDCl_3$, 300 MHz): δ 1.78 (bs, OH, 1H), 3.07 (s, 3H), 3.58 (t, 2H, J = 5.7 Hz), 3.86 (t, 2H, J = 5.7 Hz), 6.79 (d, 2H, ^3J = 8.7 Hz), 7.29 (dd, 1H, ^3J = 8.1 Hz, ^3J = 8.1 Hz), 7.42 (dd, 1H, ^3J = 8.1 Hz, ^3J = 8.1 Hz), 7.82 (d, 2H, ^3J = 8.1 Hz), 7.94 (d, 2H, ^3J = 8.7 Hz), 7.98 (d, 2H, ^3J = 8.1 Hz); ^{13}C NMR ($CDCl_3$, 75 MHz): δ 39.05, 54.67, 60.17, 111.98 (2C), 121.37 (2C), 122.15, 124.38, 126.14, 129.07 (2C); ESI/MS $C_{16}H_{16}N_2OS$ (284) m/z 284.9 $[M + H]^+$ (100%).

6-Methyl-2-[*N*-methyl-*N*-(2′-hydroxyethyl)-4′-aminophenyl]-benzothiazole (4). Compound **4** was synthesized and purified as described above for compound **3**, starting from 4-methyl-*o*-aminothiophenol (320 mg, 2.30 mmol). Yield: 60% (329 mg, 1.38 mmol); R_f = 0.43 (petroleum ether–AcOEt 1 : 1); ^{1}H NMR ($CDCl_3$, 300 MHz): δ 2.45 (s, 3H), 3.06 (s, 3H), 3.52 (t, 2H, J = 5.7 Hz), 3.85 (t, 2H, J = 5.7 Hz), 6.78 (d, 2H, ^3J = 9 Hz), 7.23 (d, 1H, ^3J = 8.1 Hz), 7.61 (s, 1H), 7.85 (d, 1H, ^3J = 8.1 Hz), 7.91 (d, 2H, ^3J = 9 Hz); ^{13}C NMR ($CDCl_3$, 75 MHz): δ 21.5, 39.0, 54.7, 60.1, 111.9 (2C); 121.2, 121.6, 127.7, 128.9, 134.5, 151.5, 168.

2-[*N*-Methyl-*N*-(2′-fluoroethyl)-4′-aminophenyl]-benzothiazole (5). To a solution of **3** (0.51 g, 1.8 mmol) in dichloromethane (10 mL) was added carbon tetrabromide (0.65 g, 1.9 mmol) at 0 °C followed by triphenylphosphine (0.517 g, 1.8 mmol). The reaction mixture was stirred for 3 h and, thereafter, the solvent was concentrated. The residue was subjected to column chromatography on silica gel (EtOAc–*n*-hexane 1 : 6) to afford **5**. Yield: 56% (350 mg, 1.0 mmol) as an yellow oil; R_f = 0.46 (AcOEt–*n*-hexane 1 : 2); ^{1}H NMR ($CDCl_3$, 300 MHz): δ 3.09 (s, 3H), 3.48 (t, 2H, J = 7.5 Hz), 3.80 (t, 2H, J = 7.5 Hz), 6.73 (d, 2H, ^3J = 8.7 Hz), 7.30 (dd, 1H, ^3J = 8.1 Hz, ^3J = 8.1 Hz), 7.43 (dd, 1H, ^3J = 8.1 Hz, ^3J = 8.1 Hz), 7.83 (d, 1H, ^3J = 8.1 Hz), 7.96 (d, 2H, ^3J = 8.7 Hz), 8.01 (d, 1H, ^3J = 8.1 Hz); ^{13}C NMR ($CDCl_3$, 75 MHz): δ 27.89, 38.87, 54.07, 111.56 (2C), 121.38, 122.27, 124.41, 126.12, 129.17 (2C), 150.11; ESI/MS $C_{16}H_{15}BrN_2S$ (346) m/z 347.0 $[M + H]^+$ (97%), 347.9 $[M + H]^+$ (20%), 348.9 $[M + H]^+$ (100%), 349.9 $[M + H]^+$ (20%).

6-Methyl-2-[*N*-methyl-*N*-(2′-fluoroethyl)-4′-aminophenyl]-benzothiazole (6). Compound **6** was synthesized and purified as described above for **5**, starting from compound **4** (300 mg, 1.00 mmol). Yield: 64% (231 mg, 0.64 mmol); R_f = 0.39 (*n*-hexane–AcOEt 1 : 4); ^{1}H NMR ($CDCl_3$, 300 MHz): δ 2.46 (s, 3H), 3.09 (s, 3H), 3.48 (t, 2H, J = 7.5 Hz), 3.80 (t, 2H, J = 7.5 Hz), 6.73 (d, 2H, ^3J = 8.7 Hz), 7.24 (d, 1H, ^3J = 8.2 Hz), 7.62 (s, 1H), 7.87 (d, 1H, ^3J = 8.2 Hz), 7.95 (d, 2H, ^3J = 8.7 Hz); ^{13}C NMR ($CDCl_3$, 75 MHz): δ 21.1, 27.7, 38.2, 53.4 (CH_2), 111.0 (2C), 120.8, 121.4, 121.7, 127.1, 128.4 (2C), 133.9, 134.2, 149.4, 151.9, 166.9; ESI/MS $C_{17}H_{17}BrN_2S$ (362) m/z 363.2.0 $[M + H]^+$.

2-[*N*-Methyl-*N*-(2′-(2″-aminoethylthio)ethyl)-4′-aminophenyl]-benzothiazole (7). To a solution of 2-aminoethanethiol hydrochloride (296 mg, 2.55 mmol) in anhydrous EtOH (8 mL) was added NaOH (163 g, 4 mmol) under a nitrogen atmosphere. After 1 h, compound **5** (448 mg, 1.29 mmol) was added and the reaction mixture was stirred for additional 20 h at room temperature. Then, the solvent was concentrated. The pallid brown residue was taken in water (25 mL) and the pH was adjusted to 7 with a 1 M HCl solution. The aqueous phase was extracted with CH_2Cl_2 (4 × 25 mL), dried over Na_2SO_4, filtered and the filtrate was concentrated. The residue was subjected to column chromatography on silica gel ($CHCl_3$–MeOH 70 : 30) to afford the desired amine as an oil. Yield: 76% (335 mg, 0.98 mmol); R_f = 0.64 ($CHCl_3$–MeOH 3 : 1); ^{1}H NMR ($CDCl_3$, 300 MHz): δ 2.68 (m, 4H), 2.87 (t, 2H, J = 6.9 Hz), 3.04 (s, 3H), 3.59 (t, 2H, J = 6.9 Hz), 6.71 (d, 2H, ^3J = 8.7 Hz), 7.28 (dd, 1H, ^3J = 7.8 Hz, ^3J = 7.2 Hz), 7.41 (dd, 1H, ^3J = 7.2 Hz, ^3J = 7.8 Hz), 7.82 (dd, 1H, ^3J = 7.8 Hz), 7.93 (d, 2H, ^3J = 8.7 Hz), 7.95 (d, 1H, ^3J = 7.8 Hz); ^{13}C NMR ($CDCl_3$, 75 MHz): δ 28.5, 36.4, 38.6, 41.1, 52.4, 111.4 (2C), 121.3, 121.5, 122.2, 124.2, 125.9, 128.9 (2C), 134.4, 150.3, 154.2, 168.5.

6-Methyl-2-[*N*-methyl-*N*-(2′-(2″-aminoethylthio)ethyl)-4′-aminophenyl]-benzothiazole (8). Compound **8** was synthesized and purified as described above for **7**, starting from compound **6** (200 mg, 0.55 mmol). Yield: 35% (68 mg, 0.19 mmol); R_f = 0.48 ($CHCl_3$–MeOH 4 : 1); ^{1}H NMR ($CDCl_3$, 300 MHz): δ 2.42 (s, 3H), 2.65 (t, 2H, J = 7.5 Hz), 2.88 (m, 2H), 2.93 (s, 3H), 3.14 (m, 2H), 3.50 (t, 2H, J = 7.5 Hz), 6.62 (d, 2H, ^3J = 9 Hz), 7.19 (d, 1H, ^3J = 8.4 Hz), 7.55 (s, 1H), 7.82 (m, 3H); ^{13}C NMR ($CDCl_3$, 75 MHz): δ 21.4, 21.3, 28.5, 29.5, 38.5, 39.2, 52.1, 111.7 (2C), 121.2, 121.6, 127.6, 128.9 (2C), 134.4, 150.3, 152.1, 167.8, 176.7.

Ethyl 2-[2′-(2″-((4‴-(benzo[*d*]thiazol-2-yl)phenyl)(methyl)-amino)ethylthio)ethylamino] acetate (9). To a solution of **7** (100 mg, 0.29 mmol), KI (1.2 mg, 7.3 μmol), and K_2CO_3 (20 mg, 0.15 mmol) in anhydrous CH_3CN (10 mL) was added ethyl 2-bromoacetate (8.2 μL, 0.145 mmol) under a nitrogen atmosphere, and the reaction mixture was refluxed overnight. Hence the solvent was concentrated. The mixture was taken in water (30 ml) and extracted with CH_2Cl_2 (3 × 30 ml). The organic phase was dried with Na_2SO_4, filtered, and the filtrate was evaporated. The residue was subjected to column chromatography on silica gel ($CHCl_3$–MeOH 95 : 5) to provide **9**. Yield: 58%. (73 mg, 0.17 mmol) as a light yellow oil; R_f = 0.55 ($CHCl_3$–MeOH 93 : 7); ^{1}H NMR ($CDCl_3$, 300 MHz): δ 1.19 (t, 3H, J = 7.2 Hz), 2.68 (m, 4H), 2.77 (t, 2H, J = 6.3 Hz), 3.00 (s, 3H), 3.36 (s, 2H), 3.55 (t, 2H, J = 6.2 Hz), 4.12 (q, 2H, J = 7.2 Hz), 6.67 (d, 2H, ^3J = 9.0 Hz), 7.23 (ddd, 1H, ^4J = 1.2 Hz, ^3J = 8.1 Hz, ^3J = 7.5 Hz), 7.36 (ddd, 1H, ^2J = 1.2 Hz, ^3J = 8.1 Hz, ^3J = 8.1 Hz), 7.77 (d, 1H, ^3J = 8.1 Hz), 7.88 (d, 2H, ^3J = 9.0 Hz), 7.90 (d, 1H, ^3J = 7.5 Hz); ^{13}C NMR ($CDCl_3$, 75 MHz): δ 14.0, 28.3, 32.4, 38.4, 47.9, 50.3, 52.2, 60.6, 111.3 (2C), 121.1, 121.3, 122.0, 124.0, 125.7, 128.8 (2C), 134.2, 150.2, 154.1, 168.4, 171.9 (C═O).

Ethyl 2-[2′-(2″-((4‴-(6⁗-methylbenzo[*d*]thiazol-2-yl)phenyl)-(methyl)amino)ethylthio)ethylamino] acetate (10). Compound **10** was synthesized and purified as described above for **9**, starting from compound **8** (55 mg, 0.15 mmol). Yield: 55% (37 mg, 0.08 mmol); R_f = 0.48 ($CHCl_3$–MeOH, 97 : 3); ^{1}H NMR ($CDCl_3$, 300 MHz): δ 1.24 (t, 3H, J = 6.9 Hz), 2.44 (s, 3H), 2.72 (m, 4H), 2.82 (t, 2H, J = 5.7 Hz), 3.03 (s, 3H), 3.40 (s, 2H), 3.59 (t, 2H, J = 7.2 Hz), 4.16 (q, 2H, J = 6.9 Hz), 6.70 (d, 2H, ^3J = 9.0 Hz), 7.23 (d, 1H, ^3J = 8.4 Hz), 7.60 (s, 1H), 7.83 (d, 1H, ^3J = 8.4 Hz), 7.91 (d, 2H, ^3J = 9.0 Hz); ^{13}C NMR ($CDCl_3$, 75 MHz): δ 14.2, 21.4, 28.6, 32.6, 38.6, 48.2, 50.3, 52.5, 60.8, 111.5 (2C), 121.1, 121.8, 127.4, 128.8 (2C), 134.2, 134.6, 150.2, 152.4, 167.5, 172.1 (C═O).

2-[*N*-Methyl-*N*-(2′-(4′-bromobutoxy)ethyl)-4′-aminophenyl]-benzothiazole (11). To a suspension of NaH (525 mg, 13.2 mmol) in anhydrous THF (40 mL) was added **3** (2.0 g, 8.05 mmol) under a nitrogen atmosphere. After 30 min, 1,4-dibromobutane (5.6 mL, 47.3 mmol) was added and the solution was left on vigorous stirring for 3 days at room temperature. Thereafter, the solvent was concentrated and the reaction

residue was subjected to column chromatography on silica gel (*n*-hexane–AcOEt 1 : 1) to afford **11**. Yield: 45% (1.518 g, 3.62 mmol); R_f = 0.54 ($CHCl_3$–MeOH 99 : 1); ^{1}H NMR ($CDCl_3$, 300 MHz): δ 1.67 (m, 2H), 1.89 (m, 2H), 3.04 (s, 3H), 3.41 (m, 4H), 3.58 (s, 4H), 6.68 (d, 2H, ^3J = 9.0 Hz), 7.23 (dd, 1H, ^3J = 7.2 Hz, ^3J = 7.8 Hz), 7.37 (d, 1H, ^3J = 7.2 Hz, ^3J = 8.1 Hz), 7.77 (d, 1H, ^3J = 7.8 Hz), 7.88 (d, 2H, ^3J = 9.0 Hz), 7.92 (d, 1H, ^3J = 8.1 Hz); ^{13}C NMR ($CDCl_3$, 75 MHz): δ 28.2, 29.6, 33.7, 39.2, 52.2, 68.2, 70.4, 111.6 (2C), 121.4, 121.9, 124.5, 126.3, 129.2, 131.9 (2C), 151.4, 164.2.

6-Methyl-(2-(*N*-methyl-*N*-(2′-(4′-bromobutoxy)ethyl)-4′-aminophenyl))-benzothiazole (12). Compound **12** was synthesized and purified as described above for **11**, starting from compound **4** (1.0 g, 3.35 mmol). Yield: 40% (581 mg, 1.34 mmol); R_f = 0.64 (*n*-hexane–AcOEt 1 : 1); ^{1}H NMR ($CDCl_3$, 300 MHz): δ 1.64 (m, 2H), 1.86 (m, 2H), 2.42 (s, 3H), 3.00 (s, 3H), 3.37 (m, 4H), 3.53 (s, 4H), 6.69 (d, 2H, ^3J = 8.7 Hz), 7.2 (d, 1H, ^3J = 8.2 Hz), 7.57 (s, 1H), 7.82 (d, 1H, ^3J = 8.2 Hz), 7.87 (d, 2H, ^3J = 8.7 Hz); ^{13}C NMR ($CDCl_3$, 75 MHz): δ 21.4, 28.1, 29.5, 33.7, 39.0, 52.0, 70.2, 111.4 (2C), 121.1, 121.3, 121.6, 127.3, 128.7 (2C), 134.1, 134.5, 150.8, 152.3, 167.6; ESI/MS $C_{21}H_{25}BrN_2OS$ (433) *m*/*z* 434.4 $[M + H]^+$.

2-[*N*-Methyl-*N*-(2′-(4″-(2‴-aminoethylthio)butoxy)ethyl)-4′-aminophenyl]-benzothiazole (13). Compound **13** was synthesized and purified as described above for **7**, starting from compound **11** (1.2 g, 2.86 mmol). Yield: 46% (547 mg, 1.32 mmol); R_f = 0.42 ($CHCl_3$–MeO 4 : 1); ^{1}H NMR (CD_3OD, 300 MHz): δ 1.62 (m, 4H), 2.51 (m, 2H), 2.63 (t, 2H, *J* = 6.6 Hz), 2.9 (t, 2H, *J* = 6.6 Hz), 3.08 (s, 3H), 3.46 (m, 2H), 3.64 (s, 4H), 6.73 (d, 2H, ^3J = 9.0 Hz), 7.28 (dd, 1H, ^3J = 7.5 Hz, ^3J = 7.8 Hz), 7.41 (dd, 1H, ^3J = 7.9 Hz, ^3J = 7.5 Hz), 7.82 (d,1H, ^3J = 7.9 Hz), 7.92 (d, 2H, ^3J = 9.0 Hz), 7.96 (d, 1H, ^3J = 7.8 Hz); ^{13}C NMR (CD_3OD, 75 MHz): δ 27.3, 29.8, 32.2, 39.3, 40.5, 52.9, 69.5, 71.7, 112.9 (2C), 122.6, 122.6, 122.7, 125.7, 127.4, 129.9 (2C), 135.3, 153.2, 155.1, 171.1.

6-Methyl-2-[*N*-methyl-*N*-(2′-(4″-(2‴-aminoethylthio)butoxy)-ethyl)-4′-aminophenyl]-benzothiazole (14). Compound **14** was synthesized and purified as described above for **7**, starting from compound **12** (900 mg, 2.08 mmol). Yield: 86% (767 mg, 1.79 mmol); R_f = 0.58 ($CHCl_3$–MeOH 3 : 1); ^{1}H NMR ($CDCl_3$, 300 MHz): δ 1.56 (m, 4H), 2.39 (s, 3H), 2.44 (m, 2H), 2.59 (t, 2H, *J* = 6.4 Hz), 2.86 (t, 2H, *J* = 6.4 Hz), 2.97 (s, 3H), 3.35 (m, 2H), 3.51 (s, 4H), 3.76 (s, 2H), 6.67 (d, 2H, ^3J = 8.8 Hz), 7.17 (d, 1H, ^3J = 8.4 Hz), 7.54 (s, 1H), 7.80 (d, 1H, ^3J = 8.4 Hz), 7.85 (d, 2H, ^3J = 8.8 Hz); ^{13}C NMR ($CDCl_3$, 75 MHz): δ 21.3, 26.1, 28.6, 31.4, 34.0, 38.8, 40.3, 52.0, 68.0, 70.6, 111.4 (2C), 121.0, 121.2, 121.5, 127.3, 128.6 (2C), 134.0; 134.4, 150.8, 152.3, 167.5; ESI/MS $C_{23}H_{31}N_3OS_2$ (429.2) *m*/*z* 430.3 $[M + H]^+$.

Ethyl 2-[4′-(benzo[*d*]thiazol-2-yl)phenyl]-5-oxa-10-thia-2,13-diazapentadecan-15-oate (15). Compound **15** was synthesized and purified as described above for **9**, starting from compound **13** (500 mg, 1.20 mmol). Yield: 66% (397 mg, 0.79 mmol); R_f = 0.53 ($CHCl_3$–MeOH 95 : 5); ^{1}H NMR ($CDCl_3$, 300 MHz): δ 1.23 (t, 3H, *J* = 7.2 Hz), 1.61 (m, 4H), 2.50 (m, 2H), 2.62 (t, 2H, *J* = 6.2 Hz), 2.77 (t, 2H, *J* = 6.2 Hz), 3.04 (s, 3H), 3.40 (m, 4H), 3.57 (s, 4H), 4.15 (q, 2H, *J* = 7.2 Hz), 6.72 (d, 2H, ^3J = 9.0 Hz), 7.26 (dd, 1H, ^3J = 7.2 Hz, ^3J = 7.8 Hz), 7.40 (dd, 1H, ^3J = 7.2 Hz, ^3J = 8.1 Hz), 7.80 (dd, 1H, ^4J = 0.6 Hz, ^3J = 7.8 Hz), 7.90 (d, 2H, ^3J = 9.0 Hz), 7.94 (d, 1H, ^3J = 8.1 Hz); ^{13}C NMR ($CDCl_3$, 75 MHz): δ 13.9, 25.9, 28.5, 31.2, 31.4, 38.8, 47.4, 49.8, 51.8, 60.6, 67.8, 70.5, 111.2 (2C), 120.8, 121.1, 121.9, 123.9, 125.7, 128.6 (2C), 134.1, 150.8, 154.0, 168.5, 171.5 (C═O); ESI/MS $C_{26}H_{35}N_3O_3S_2$ (501.2) *m*/*z* 502.4 $[M + H]^+$.

Ethyl 2-[4′-((6″-methyl)benzo[*d*]thiazol-2-yl)phenyl]-5-oxa-10-thia-2,13-diazapentadecan-15-oate (16). Compound **16** was synthesized and purified as described above for **9**, starting from compound **14** (700 mg, 1.63 mmol). Yield: 36% (303 mg, 0.59 mmol); R_f = 0.41 ($CHCl_3$–MeOH 97 : 3); ^{1}H NMR ($CDCl_3$, 300 MHz): δ 1.23 (t, 3H, *J* = 7.2 Hz), 1.60 (m, 4H), 2.42 (s, 3H), 2.49 (m, 2H), 2.61 (t, 2H, *J* = 6.3 Hz), 2.76 (t, 2H, *J* = 6.3 Hz), 3.02 (s, 3H), 3.39 (m, 4H), 3.55 (s, 4H), 4.14 (q, 2H, *J* = 7.2 Hz), 6.70 (d, 2H, ^3J = 9.0 Hz), 7.20 (d, 1H, ^3J = 8.4 Hz), 7.58 (s, 1H), 7.82 (d, 1H, ^3J = 8.1 Hz), 7.88 (d, 2H, ^3J = 9.0 Hz); ^{13}C NMR ($CDCl_3$, 300 MHz): δ 13.2, 20.5, 25.2, 27.8, 30.2, 30.7, 38.1, 46.9, 48.8, 51.2, 60.3, 67.2, 69.8, 110.6 (2C), 120.2, 120.5, 120.8, 126.5, 127.8 (2C), 133.2, 133.7, 150.0, 151.5, 166.7; ESI/MS $C_{27}H_{37}N_3O_3S_2$ (515.2) *m*/*z* 516.3 $[M + H]^+$.

2-[(2-((2″-((4″-(Benzo[*d*]thiazol-2-yl)phenyl)(methyl)amino)-ethyl)thio]ethyl)amino) acetic acid (L1). A solution of **9** (148 mg, 0.35 mmol) in THF (10 mL) and water (15 mL) was refluxed with NaOH (136 mg, 3.40 mmol) for 17 h. After cooling down, the reaction mixture was neutralized with 1 M HCl, followed by extraction with $CHCl_3$ (2 × 25 mL). The organic phase was dried over Na_2SO_4, filtered and the filtrate was concentrated. Recrystallization of the precipitate in methanol afforded **L1** as a white solid. Yield: 58% (80 mg, 0.20 mmol); R_f = 0.29 ($CHCl_3$–MeOH 3 : 1); ^{1}H NMR (DMSO, 300 MHz): δ 2.80 (m, 4H), 2.98 (t, 2H, *J* = 8.1 Hz), 3.03 (s, 3H), 3.21 (s, 2H), 3.62 (t, 2H, *J* = 8.1 Hz), 6.84 (d, 2H, ^3J = 9.0 Hz), 7.39 (ddd, 1H, ^4J = 1.2 Hz, ^3J = 7.8 Hz, ^3J = 7.5 Hz), 7.51 (ddd, 1H, ^4J = 1.2 Hz, ^3J = 7.5 Hz, ^3J = 8.1 Hz), 7.89 (d, 2H, ^3J = 9.0 Hz), 7.92 (d, 1H, ^3J = 8.1 Hz), 8.04 (d, 1H, ^3J = 7.8 Hz); ^{13}C NMR (DMSO, 75 MHz): δ 25.7, 46.4, 49.6, 51.3, 56.1, 111.8 (2C), 120.3, 122.0, 124.5, 126.4, 128.7 (2C), 133.8, 150.7, 153.9, 167.8; ESI/MS $C_{20}H_{23}N_3O_2S_2$ (401.55) *m*/*z* 402.2 $[M + H]^+$, 424.2 $[M + Na]^+$; Anal. calcd for $C_{20}H_{23}N_3O_2S_2{\cdot}1.4H_2O$: C 56.38, H 6.09, N 9.86; found C 56.54, H 6.15, N 9.61.

2-[2′-(2″-((4‴-(6⁗-Methylbenzo[*d*]thiazol-2-yl)phenyl)(methyl)-amino)ethylthio)ethylamino] acetic acid (L2). L2 was synthesized and purified as described above for **L1**, starting from compound **10** (30 mg, 0.067 mmol). Yield: 65% (18 mg, 0.04 mmol); ^{1}H NMR (CD_3OD, 300 MHz): δ 2.46 (s, 3H), 3.09 (s, 2H), 2.85 (m, 4H), 3.42 (s, 3H), 3.69 (m, 4H), 6.84 (d, 2H, ^3J = 9.0 Hz), 7.28 (d, 1H, ^3J = 8.4 Hz), 7.70 (s, 1H), 7.76 (d, 1H, ^3J = 8.4 Hz), 7.87 (d, 2H, ^3J = 9.3 Hz); ^{13}C NMR (CD_3OD, 75 MHz): δ 22.5, 25.3, 28.3, 29.2, 37.8, 67.7, 111.7 (2C), 121.0, 121.2, 127.7, 128.7 (2C), 134.9; ESI/MS $C_{21}H_{25}N_3O_2S_2$ (415.14) *m*/*z* 416.3 $[M + H]^+$, 438.3 $[M + Na]^+$; Anal. calcd for $C_{21}H_{25}N_3O_2S_2{\cdot}1.6H_2O$: C 56.75, H 6.12, N 9.46; found C 55.98, H 6.48, N 9.27.

[4-(Benzo[*d*]thiazol-2-yl)phenyl]-5-oxa-10-thia-2,13-diazapentadecan-15-oic acid (L3). L3 was synthesized and purified as described above for **L1**, starting from compound **15** (350 mg,

0.70 mmol). Yield: 52% (172 mg, 0.36 mmol); ^{1}H NMR (CD_3OD, 300 MHz): δ 1.63 (m, 4H), 2.55 (t, 2H, J = 7.2 Hz), 2.75 (t, 2H, J = 7.2 Hz), 3.08 (s, 3H), 3.14 (t, 2H, J = 6.9 Hz), 3.47 (m, 4H), 3.64 (s, 4H), 6.86 (d, 2H, ^3J = 7.2 Hz), 7.34 (ddd, 1H, ^3J = 7.8, 7.5 Hz, ^4J = 1.2, 0.6 Hz), 7.46 (td, 1H, ^3J = 7.8; 7.5 Hz, ^4J = 1.2; 0.6 Hz), 7.89 (m, 4H); ^{13}C NMR (CD_3OD, 75 MHz): δ 27.1, 28.6, 29.8, 32.1, 39.3, 52.9, 66.9, 69.5, 71.7, 112.9 (2C), 121.6, 122.6, 122.7, 125.7, 127.4, 129.9 (2C), 135.3, 153.2, 155.1, 171.1 (C═O); ESI/MS $C_{24}H_{31}N_3O_3S_2$ (473.18) m/z 472.2 $[M - H]^+$; Anal. calcd for $C_{24}H_{31}N_3O_3S_2{\cdot}2.2H_2O$: C 56.16, H 6.95, N 8.19; found C 56.63, H 7.09, N 8.02.

2-[4′-((6″-Methyl)benzo[*d*]thiazol-2-yl)phenyl]-5-oxa-10-thia-2,13-diazapentadecan-15-oic acid (L4). L4 was synthesized and purified as described above for **L1**, starting from compound **16** (250 mg, 0.48 mmol). Yield: 65% (154 mg, 0.32 mmol); ^{1}H NMR (CD_3OD, 300 MHz): δ 1.60 (m, 4H), 2.52 (t, 2H, J = 7.2 Hz), 2.74 (t, 2H, J = 7.2 Hz), 3.06 (s, 2H), 3.12 (t, 2H, J = 7.2 Hz), 3.45 (s, 3H), 3.62 (s, 4H), 6.80 (d, 2H, ^3J = 9.0 Hz), 7.24 (d, 1H, ^3J = 8.4 Hz), 7.68 (s, 1H), 7.72 (d, 1H, ^3J = 8.4 Hz), 7.82 (d, 2H, ^3J = 9.0 Hz); ^{13}C NMR (CD_3OD, 75 MHz): δ 27.5, 28.9, 30.1, 32.5, 39.7, 53.4, 67.3, 69.9, 72.1, 112 (2C), 123.0, 123.2, 129.8, 129.0 (2C), 135.2.2, 153.4, 155.3, 171.4 (C═O); ESI/MS $C_{25}H_{33}N_3O_3S_2$ (487.2) m/z 488.4 $[M + H]^+$, 510.4 $[M + Na]^+$. Anal. calcd for $C_{25}H_{33}N_3O_3S_2{\cdot}1.5H_2O$: C 58.34, H 6.75, N 8.17; found C 57.24, H 6.88, N 8.24.

General procedure for the synthesis of the rhenium complexes (Re1–Re4)

fac-$[Re(H_2O)_3(CO)_3]Br$ was reacted with equimolar amounts of **L1–L4** in refluxing methanol for 16 h. Thereafter, the solvent was removed under vacuum and the desired complexes were purified by successive washing with water, diethyl ether and *n*-hexane. The obtained yellow solids were further recrystallized from methanol to afford pure samples of **Re1–Re4**, as checked by HPLC analysis.

Re1 was obtained in 62% yield (54 mg, 0.08 mmol); ^{1}H NMR (DMF-d_7, 300 MHz, T = 20 °C): 2.64 (m, 2H), 3.20 (s, 4H), 3.38 (m, 2H), 3.71 (m, 2H), 3.96 (m, 2H), 7.05 (d, 2H, J = 9.0 Hz), 7.40 (m, 1H), 7.52 (m, 1H), 7.98 (m, 3H), 8.10 (d, 1H, J = 7.8 Hz); ^{13}C NMR (DMF-d_7, 300 MHz, T = 20 °C): δ 39.1, 51.50, 53.32, 54.40, 55.43, 56.40, 113.09, 113.47, 122.93, 123.27, 125.64, 127.40, 129.95, 135.60, 152.30, 155.71, 169.13, 180.16, 193.72, 197.17; IR (KBr) ν: 3410, 2922, 1894, 1699, 1606, 1486, 1455, 1384, 1261, 1191, 1104, 817 cm^{-3}; ESI/MS (+) $C_{23}H_{22}N_3O_5S_2Re$ (671.0) (m/z): 672.2 $[M + H]^+$ (100); Anal. calcd for $C_{23}H_{22}N_3O_5S_2Re$: C 41.18, H 3.31, N 6.27; found C 41.07, H 3.47, N 6.19.

Re2 was obtained in 57% yield (32 mg, 0.05 mmol); ^{1}H NMR (DMF-d_7, 300 MHz, T = 20 °C): δ 2.47 (m, 6H), 3.19 (s, 9H), 6.99 (s, 2H), 7.32 (s, 1H), 7.83 (m, 2H), 7.95 (m, 2H); ^{13}C NMR (DMF-d_7, 300 MHz, T = 20 °C): δ 21.18, 32.33, 38.51, 38.66, 47.99, 50.39, 50.83, 52.65, 54.30, 54.95, 55.66, 55.96, 112.36, 112.72, 121.41, 122.09, 128.35, 129.17, 134.90, 135.24, 151.32, 152.88, 167.69, 181.17, 192.76, 196.56, 198.16; IR (KBr) ν: 3395, 2924, 2028, 1893, 1700, 1604, 1509, 1483, 1437, 1384, 1261, 1193, 1108, 817, 759, 698, 650 cm^{-3}; ESI/MS (+) $C_{24}H_{24}N_3O_5S_2Re$ (685.07) (m/z) 686.3 $[M + H]^+$ (100); Anal. calcd for $C_{24}H_{24}N_3O_5S_2Re$: C 42.09, H 3.53, N 6.14; found C 42.25, H 3.75, N 6.09.

Re3 was obtained in 76% yield (78 mg, 0.11 mmol); ^{1}H NMR (DMF-d_7, 300 MHz, T = 20 °C): δ 1.71 (m, 4H), 3.08 (s, 4H), 3.50 (s, 3H), 3.65 (m, 5H), 6.90 (d, 2H, J = 8.4 Hz), 7.39 (m, 1H), 7.50 (m, 1H), 7.95 (m, 3H); ^{13}C NMR (DMF-d_7, 300 MHz, T = 20 °C): δ 25.01, 28.32, 37.10, 38.54, 51.53, 53.74, 55.76, 68.13, 70.10, 111.90, 120.18, 121.82, 121.97, 124.78, 126.56, 128.79, 134.10, 151.86, 154.14, 168.93, 181.51, 192.31, 196.12, 197.75; IR (KBr) ν: 4008, 2923, 2027, 1896, 1748, 1606, 1559, 1541, 1508, 1487, 1456, 1384, 1350, 1261, 1183, 1101, 816, 691, 651, 567, 516 cm^{-3}; ESI/MS (+) $C_{27}H_{30}N_3O_6S_2Re$ (743.0) (m/z) 744.4 $[M + H]^+$, 766.4 $[M + Na]^+$; Anal. calcd for $C_{27}H_{30}N_3O_5S_2Re$: C 43.65, H 4.07, N 5.66; found C 43.48, H 4.24, N 5.54.

Re4 was obtained in 81% yield (86 mg, 0.11 mmol); ^{1}H NMR (DMF-d_7, 400 MHz, T = 20 °C): 1.74 (s, 2H), 1.83 (s, 2H), 2.47 (s, 3H), 3.12 (s, 5H), 3.41 (q, 2H, J = 3.2 Hz), 3.52 (s, 2H), 3.68 (s, 5H), 6.93 (d, 2H, J = 7.4 Hz), 7.33 (s, 1H), 7.85 (m, 2H), 7.94 (d, 2H, J = 7.4 Hz); ^{13}C NMR (DMF-d_7, 400 MHz, T = 20 °C): δ 15.94, 21.68. 26.28, 35.02, 35.23, 37.86, 39.30, 39.59, 52.69, 54.80, 56.08, 66.38, 69.19, 71.13, 112.90, 121.80, 122.65, 128.79, 129.61, 135.52, 152.61, 153.55, 168.26, 171.92, 177.35, 180.44, 194.18, 197.49; IR (KBr) ν: 3490, 2920, 2028, 1895, 1653, 1606, 1558, 1506, 1457, 1384, 1261, 1100, 921, 688 cm^{-3}; ESI/MS (+) $C_{28}H_{32}N_3O_6S_2Re$ (757.0) (m/z) 758.6 $[M + H]^+$ (100), 780.5 $[M + Na]^+$ (80); Anal. calcd for $C_{28}H_{32}N_3O_6S_2Re$: C 44.43, H 4.26, N 5.55; found C 43.97, H 4.6, N 5.43.

General procedure for the synthesis of ^{99m}Tc complexes

In a nitrogen-purged glass vial, 120 μL of a 1.1 × 10^{-3} M solution of **L1–L4** in propanediol-1,3 was added to 1.2 mL of a solution of the organometallic precursor *fac*-$[^{99m}Tc(H_2O)_3(CO)_3]^+$ (1–2 mCi) in saline at pH 7.4. The reaction mixtures were then heated to 100 °C for 30 min, cooled to room temperature and analyzed by RP-HPLC, using the method described above. Following this procedure, all ^{99m}Tc complexes (**Tc1–Tc4**) were synthesized in radiochemical yields >95% without the need for further purification. Their chemical identity was ascertained by HPLC comparison with the Re congeners (see Table 1).

Determination of partition coefficients

The log $D_{o/w}$ values of complexes **Tc1–Tc2** were determined by the "shake flask" method.[28] A mixture of octanol (1 mL) and 0.1 M PBS pH = 7.4 (1 mL) was stirred vigorously, followed by the addition of 25 μL of the aqueous solutions of each complex. The mixtures were vortexed and centrifuged (3000 rpm, 10 min, RT) to allow phase separation. Aliquots of 25 μL of the octanol and PBS phases were counted in a gamma counter. The partition coefficient ($P_{o/w}$) was calculated by dividing the number of counts of the octanol phase by those from the PBS phase, and the results are expressed as log $D_{o/w}$.

Cell culture

The human MCF7 breast and PC3 prostate cells (American Type Culture Collection, ATCC) were grown respectively in DMEM and RPMI media, supplemented with 10% (v/v) fetal bovine serum and 1% penicillin–streptomycin (all from Invitrogen). Cells were cultured at 37 °C in a 5% CO_2 incubator (Heraus, Germany) under a humidified atmosphere, with the medium changed every other day.

Cytotoxicity assays

The cell viability was evaluated by using a colorimetric method based on the tetrazolium salt MTT ([3-(4,5-dimethylthiazol-2-yl)-2,5-diphenyltetrazolium bromide]), which is reduced by living cells to yield purple formazan crystals. Cells were seeded in 96-well plates at a density of 1–1.5 × 10^4 cells per well in 200 μL of culture medium and incubated overnight. After careful removal of the medium, 200 μL of a dilution series of the compounds in fresh medium were added and incubation was performed at 37 °C/5% CO_2 for 72 h. The percentage of DMSO in cell culture medium did not exceed 1%. At the end of the incubation period, the compounds were removed and the cells were incubated with 200 μL of MTT solution (500 μg ml^{-1}). After 3 h, the medium was removed and the purple formazan crystals were dissolved in 200 μL of DMSO by shaking. The cell viability was evaluated by the measurement of the absorbance at 570 nm using a plate spectrophotometer (Power Wave Xs, Bio-Tek). The cell viability was calculated by the ratio between the absorbance of each well and that of the control wells (cells treated with medium containing 1% DMSO). Each experiment was repeated at least three times and each point was determined in at least six replicates. Data were analyzed with GraphPad Prism software.

Fluorescence spectra and fluorescence microscopy analysis

The excitation and emission wavelengths of **L3** and **Re3** (25 μM in PBS) were recorded using a plate reader (Tecan Infinite 200, Männedorf, Switzerland). The maximum excitation and emission wavelengths were determined according to the maximum fluorescence intensity level.

MCF7 and PC3 cells, cultured in 35 mm imaging dishes (Ibidi), were treated with a vehicle (DMSO) or with the ligands **L3** or the complex **Re3** (100 μM), for 24 h. Cells washed with PBS were fixed and permeabilized in 100% ice-cold methanol (−20 °C, 5 min). Cells, washed with PBS 3 times, were incubated with 20 μg ml^{-1} propidium iodide (nuclear staining) for 4 min at RT. Cells were washed with PBS 3 times and were kept at 4 °C until analysis. Samples were imaged on a widefield fluorescence microscope Zeiss Axiovert 200M (Carl Zeiss MicroImaging) using a 63× Plan-Apochromat using the Red (λ_{ex} = 540–552 nm, λ_{em} = 575–640 nm) and Blue (λ_{ex} = 359–371 nm, λ_{em} > 397 nm) filter sets. Images were acquired using a cooled CCD camera (Roper Scientific Coolsnap HQ CCD) using Zeiss Metamorph software. All images were processed using ImageJ – Image Processing and Analysis in Java.[29]

Cellular uptake

Cellular uptake assays of the ^{99m}Tc complexes (**Tc1–Tc4**) were performed using PC-3 and MCF-7 cells seeded at a density of 4 × 10^4 cells in 500 μL medium per well in 24-well plates and allowed to attach overnight. After that period, the medium was removed and cells were treated with fresh medium containing approximately 25 kBq mL^{-1} of each ^{99m}Tc complex and incubated under a humidified 5% CO_2 atmosphere, at 37 °C for a period of 30 min to 18 h. Cells were washed twice with cold PBS, lysed with 0.1 M NaOH and the cellular extracts were analyzed for radioactivity. Each experiment was performed in duplicate with each point determined in at least four replicates. Cellular uptake data were expressed as an average plus the standard deviation of % of total per million of cells.

Biodistribution studies

All animal experiments were performed in compliance with Portuguese regulations for animal treatment. The animals were housed in a temperature- and humidity-controlled room with a 12 h light/12 h dark schedule. Biodistribution of complexes **Tc1–Tc4** was evaluated in CD-1 mice (randomly bred, obtained from IFFA, CREDO, Spain) weighing approximately 20–25 g. Animals were intravenously injected in the tail vein with the test complex (1.8–7.8 MBq) diluted in 100 μL of NaCl 0.9%. Mice were sacrificed by cervical dislocation at 2 min and 1 h after injection. The administered dose and the radioactivity in the sacrificed animals were measured using a dose calibrator (Curiemeter IGC-3, Aloka, Tokyo, Japan). The difference between the radioactivity in the injected and sacrificed animals was assumed to be due to excretion. The tissues of interest were dissected, rinsed to remove excess blood, weighed, and their radioactivity was measured using a γ-counter (LB2111, Berthold, Germany). The uptake in the tissues was calculated and expressed as a percentage of the injected radioactivity dose per gram of tissue.

In vivo stability studies

The *in vivo* stability of **Tc1–Tc4** was evaluated by urine and blood serum HPLC analysis, using the elution conditions above described for the analysis of these ^{99m}Tc complexes. The urine was collected at the sacrifice time and centrifuged for 5 min at 1500*g* before RP-HPLC analysis. Blood collected from mice was also centrifuged for 10 min at 1000*g* at 4 °C, and the supernatant (serum) was collected. Aliquots of 100 μL of serum were treated with 200 μL of cold ethanol for protein precipitation. Samples were centrifuged at 1500*g* for an additional 10 min, at 4 °C. The remaining supernatant was separated and injected through a RP-HPLC column (Nucleosil 100-10, 250 × 3 mm) for analysis.

Acknowledgements

This work was funded by the Fundação para a Ciência e Tecnologia (FCT), Portugal (EXCL/QEQ-MED/0233/2012). The research was carried out within the framework of the European

Cooperation COST Action CM1105. FCT is also acknowledged for "Ciência 2008" program (GRM), FCT Investigator Grant (FM) and grants SFRH/BPD/80758/2011 (EP), SFRH/BD/47308/2008 (FS) and SFRH/BPD/64702/2009 (HVM). TFO is supported by the DFG Center for Nanoscale Microscopy and Molecular Physiology of the Brain (CNMPB). The authors thank Dr Joaquim Marçalo and Dr Célia Fernandes for Mass Spectroscopy analysis, which was carried out on a QITMS instrument, acquired with the support of the Programa Nacional de Reequipamento Científico (Contract REDE/1503/REM/2005-ITN) of FCT and is part of RNEM-Rede Nacional de Espectrometria de Massa.

Notes and references

1 I. Hutchinson, M.-S. Chua, H. L. Browne, V. Trapani, T. D. Bradshaw, A. D. Westwell and M. F. G. Stevens, *J. Med. Chem.*, 2001, **44**, 1446.
2 X. Peng, G. Xie, Z. Wang, H. Lin, T. Zhou, P. Xiang, Y. Jiang, S. Yang, Y. Wei, L. Yu and Y. Zhao, *Cell Death Dis.*, 2014, **5**, e1143.
3 G. R. Morais, A. Paulo and I. Santos, *Eur. J. Org. Chem.*, 2012, 1279.
4 W. E. Klunk, H. Engler, A. Nordberg, Y. Wang, G. Blomqvist, D. P. Holt, M. Bergstrom, I. Savitcheva, G. F. Huang, S. Estrada, B. Ausen, M. L. Debnath, J. Barletta, J. C. Price, J. Sandell, B. J. Lopresti, A. Wall, P. Koivisto, G. Antoni, C. A. Mathis and B. Langstrom, *Ann. Neurol.*, 2004, **55**, 306.
5 H. Engler, A. Forsberg, O. Almkvist, G. Blomquist, E. Larsson, I. Savitcheva, A. Wall, A. Ringheim, B. Langstrom and A. Nordberg, *Brain*, 2006, **129**, 2856.
6 S. M. Landau, B. A. Thomas, L. Thurfjell, M. Schmidt, R. Margolin, M. Mintun, M. Pontecorvo, S. L. Baker and W. Jagust, *Eur. J. Nucl. Med.*, 2014, **41**, 1398.
7 S. Iikuni, M. Ono, H. Watanabe, K. Matsumura, M. Yoshimura, N. Harada, H. Kimura, M. Nakayama and H. Saji, *Mol. Pharmaceutics*, 2014, **11**, 1132.
8 J. Jia, M. Cui, J. Dai, X. Wang, Y.-S. Ding, H. Jia and B. Liu, *Med. Chem. Commun.*, 2014, **5**, 153.
9 A. F. Martins, J. F. Morfin, A. Kubickova, V. Kubicek, F. Buron, F. Suzenet, M. Salerno, A. N. Lazar, C. Duyckaerts, N. Arlicot, D. Guilloteau, C. F. G. C. Geraldes and E. Toth, *ACS Med. Chem. Lett.*, 2013, **4**, 436.
10 T. D. Bradshaw and A. D. Westwell, *Curr. Med. Chem.*, 2004, **11**, 1241.
11 C. G. Mortimer, G. Wells, J.-P. Crochard, E. L. Stone, T. D. Bradshaw, M. F. G. Stevens and A. D. Westwell, *J. Med. Chem.*, 2006, **49**, 179.
12 A. I. Loaiza-Pérez, V. Trapani, C. Hose, S. S. Singh, J. B. Trepel, M. F. G. Stevens, T. D. Bradshaw and E. A. Sausville, *Mol. Pharmacol.*, 2002, **61**, 13.
13 V. Trapani, V. Patel, C.-O. Leong, H. P. Ciolino, G. C. Yeh, C. Hose, J. B. Trepel, M. F. G. Stevens, E. A. Sausville and A. I. Loaiza-Pérez, *Br. J. Cancer*, 2003, **88**, 599–605.
14 E. W. Price and C. Orvig, *Chem. Soc. Rev.*, 2014, **43**, 260.
15 C.-T. Yang and K.-H. Chuang, *Med. Chem. Commun.*, 2012, **3**, 552–565.
16 S. Tzanopoulou, I. C. Pirmettis, G. Patsis, M. Paravatou-Petsotas, E. Livaniou, M. Papadopoulos and M. Pelecanou, *J. Med. Chem.*, 2006, **49**, 5408.
17 S. Tzanopoulou, M. Sagnou, M. Paravatou-Petsotas, E. Gourni, G. Loudos, S. Xanthopoulos, D. Lafkas, H. Kiaris, A. Varvarigou, I. C. Pirmettis, M. Papadopoulos and M. Pelecanou, *J. Med. Chem.*, 2010, **53**, 4633.
18 H. K. Kim, M. K. Kang, K. H. Jung, S. H. Kang, Y. H. Kim, J. C. Jung, G. H. Lee, Y. Chang and T. J. Kim, *J. Med. Chem.*, 2013, **56**, 8104.
19 R. Alberto, R. Schibli, A. Egli and A. P. Schubiger, *J. Am. Chem. Soc.*, 1998, **120**, 7987.
20 R. Alberto, K. Ortner, N. Wheatley, R. Schibli and A. P. Schubiger, *J. Am. Chem. Soc.*, 2001, **123**, 3135.
21 G. R. Morais, A. Paulo and I. Santos, *Organometallics*, 2012, **31**, 5693.
22 C. Moura, L. Gano, I. C. Santos, I. Santos and A. Paulo, *Eur. J. Inorg. Chem.*, 2011, 5405.
23 C. Moura, L. Gano, F. Mendes, P. D. Raposinho, A. M. Abrantes, M. F. Botelho, I. Santos and A. Paulo, *Eur. J. Med. Chem.*, 2012, **50**, 350.
24 I. Fichtner, A. Monks, C. Hose, M. F. G. Stevens and T. D. Bradshaw, *Breast Cancer Res. Treat.*, 2004, **87**, 97.
25 C. Fernandes, L. Maria, L. Gano, I. C. Santos, I. Santos and A. Paulo, *J. Organomet. Chem.*, 2014, **760**, 138.
26 M. Q. Zheng, D. Z. Yin, J. P. Qiao, L. Zhang and Y. X. Wang, *J. Fluorine Chem.*, 2008, **129**, 210.
27 N. Lazarova, S. James, J. Babich and J. Zubieta, *Inorg. Chem. Commun.*, 2004, **7**, 1023.
28 D. E. Troutner, W. A. Volkert, T. J. Hoffman and R. A. Holmes, *Int. J. Appl. Radiat. Isot.*, 1984, **35**, 467.
29 M. D. Abramoff, P. J. Magelhaes and S. J. Ram, *Biophotonics Int.*, 2004, 11.

